Nanoprotective Layer-by-Layer Coatings with Epoxy Components for Enhancing Abrasion Resistance: Toward Robust Multimaterial Nanoscale Films

Shahid Saeed Qureshi,[†,‡,∥,▽] Zhiqiang Zheng,[†,#,▽] Muhammad Ilyas Sarwar,[‡] Olivier Félix,[†] and Gero Decher[†,§,⊥,*]

[†]C.N.R.S., Institut Charles Sadron, 23 rue du Loess, F-67034 Strasbourg, France, [‡]Department of Chemistry, Quaid-i-Azam University, Islamabad - 45320, Pakistan, [§]Université de Strasbourg, Faculté de Chimie, 1 rue Blaise Pascal, F-67008 Strasbourg, France, and [⊥]International Center for Frontier Research in Chemistry, 8 allée Gaspard Monge, F-67083 Strasbourg, France. [▽]These authors contributed equally. [∥]Present address: Government College, G.T. Road Jhelum, Pakistan. [#]Present address: BASF SE, Carl-Bosch Str. 38, D-67056 Ludwigshafen, Germany.

ABSTRACT Layer-by-Layer (LbL) assembled films offer many interesting applications (*e.g.*, in the field of nanoplasmonics), but are often mechanically feeble. The preparation of nanoprotective films of an oligomeric novolac epoxy resin with poly(ethyleneimine) using covalent LbL-assembly is described. The film growth is linear, and the thickness increment per layer pair is easily controlled by varying the polymer concentration and/or the adsorption times. The abrasion resistance of such cross-linked films was tested using a conventional rubbing machine and found to be greatly enhanced in comparison to that of classic LbL-films that are mostly assembled through electrostatic interactions. These robust LbL-films are then used to mechanically protect LbL-films that would completely be removed by a few rubbing cycles in the absence of a protective coating. A 45 nm thick LbL-film composed of gold nanoparticles and poly(allylamine hydrochloride) was chosen as an especially weak example for a functional multilayer system. The critical thickness for the protective LbL-coatings on top of the weak multilayer was determined to be about 6 layer pairs corresponding to about only 10 nm. At this thickness, the whole film withstands at least 25 abrasion cycles with a reduction of the total thickness of only about 2%.

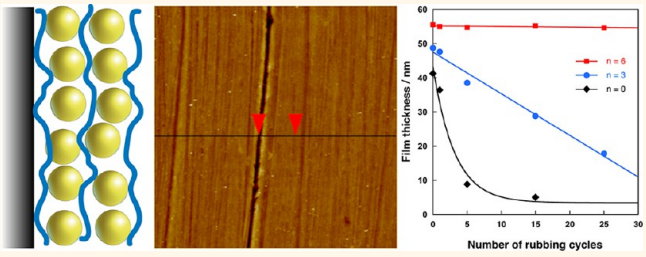

KEYWORDS: Layer-by-Layer assembly · multilayer films · epoxy resin · wear protection · abrasion resistance · chemical cross-linking · ultrathin coatings

The development of new materials, in particular composite materials, has increasingly focused on engineering techniques at the nanoscale, both with respect to fundamental science and to potential applications. A particularly successful method for the functionalization of surfaces and the preparation of nanoscale hybrid films is the Layer-by-Layer (LbL) assembly technique developed by Decher and coworkers in the 1990s.[1,2] The wealth of different potential applications is due to the fact that Layer-by-Layer assembly can be used with an unprecedented choice of different components and that even films with complex functionality/architecture are easily prepared using a single process that can be adapted to a large variety of surfaces. In many cases, it offers ease of application even on large surfaces, nanoscale precision of the multilayer architecture and very high reproducibility. LbL-assembly is usually performed in aqueous media and typically involves the consecutively alternating adsorption of oppositely charged molecules, such as polyelectrolytes or objects such as nanoparticles. Nowadays, it can be considered routine to incorporate biological,[3] metallic[4] or oxidic[5] nanoparticles, nanoplatelets,[6,7] DNA,[8] therapeutic compounds,[9−11]

* Address correspondence to decher@unistra.fr.

Received for review August 2, 2013 and accepted September 16, 2013.

Published online September 16, 2013
10.1021/nn4040298

and carbon nanotubes,[12] among other components, either individually or as a mixture of different materials, into LbL-assembled films. While most LbL-films are prepared employing electrostatic interactions, other interactions are used as well including covalent bond formation (see for example refs 11, 13−24).

An important drawback in the field of very thin coatings is that almost any film partially or totally composed of organic or polymeric constituents lacks the mechanical robustness of some of its inorganic counterparts. More durable films composed of "soft matter" components such as paints, typically require a thickness in the micrometer range to be mechanically robust or to have a reasonable scratch resistance. However, for applications in thin film devices, it is often sufficient to possess a good abrasion resistance, especially if the protective coating can be applied at low cost. Particularly interesting are coatings that do not require the use of vacuum equipment or treatment at elevated temperatures. For a large number of devices, functional films are never exposed to the environment and are only required to withstand handling during the assembly of the final device. For such a purpose, even very thin polymeric films can offer sufficient mechanical protective strength.

There are only very few reports in the past on how to prepare LbL-films with good abrasion resistance[25] or on durable LbL-films.[26] We have therefore investigated if LbL-assembled films can be rendered mechanically more robust by applying a protective coating against mechanical abrasion on top of a functional LbL-film. To have good adhesion to the functional film and to avoid switching to a different deposition process for applying the protective coating, all steps for building the entire film architecture should be based on Layer-by-Layer assembly. With the work described below, we are focusing on the question how many LbL-strata of components with excellent toughness (epoxy resins) will be needed for protecting even mechanically weak LbL-films and which minimum film thickness is required for doing so. In this context it is highly important to optimize the fabrication of a nanoprotective coating with respect to the shortest possible deposition time for a protective multilayer system through the best combination of the adsorption time per layer and the total number of protective layers.

As a model for a functional film with poor mechanical properties, gold nanoparticles (AuNPs) and poly(allylamine hydrochloride) (PAH) were selected as film components. The gold nanoparticles in such a LbL-film show a plasmon absorbance in the visible which depends on the chemical composition of the environment surrounding the particles and which can thus be used for detecting structural changes in the functional film. We have reported previously on the optical properties of such films prepared by "dipping";[4] here we are using spray-assisted LbL-assembly for speeding up the deposition of $(PAH/AuNP)_n$ films. Another important reason for using this type of functional film is that it is exceptionally weak and easily rubbed off from a smooth surface even with tissue paper or a soft textile. Without protection, such $(PAH/AuNP)_n$ films must always be handled with great care in order to prevent accidental abrasion of the film.

Polyepoxides are thermally cured copolymers composed of an epoxy "resin" and a polyamine "hardener". They belong to the class of structural adhesives and are well-known for their excellent properties including electrical insulation or chemical, heat and mechanical resistance. The major application of epoxy resins is as coatings and adhesives.[27] Even though epoxy resins are usually dissolved in organic solvents, they can also be used for the covalent coupling with water-soluble compounds including biological ones.[28] Epoxy-based components have already been used in Layer-by-Layer assembled films.[29,30] Oligo- or polymeric amines have previously been used for the assembly of LbL-films, whereas the second component, oligo- or polymeric epoxy derivatives, have only be sparsely been used in this context. In combination, both components ensure the formation of densely cross-linked materials, some of whose properties are controlled by the curing temperature. We have chosen an epoxy novolac resin which is known to provide excellent chemical resistance associated with an increased cross-link density when used in a solvent or waterborne formulation. As amine component we have chosen poly(ethyleneimine) because it carries primary and secondary amino groups and because it can conveniently be employed as interfacial layer between electrostatically assembled and covalently deposited strata of a LbL-film or -device.

RESULTS AND DISCUSSION

After screening a selection of different commercial oligo- and polymeric resins and hardeners, a branched poly(ethyleneimine) (PEI) was selected as amino component and poly[(*o*-cresyl glycidyl ether)-*co*formaldehyde] (Cresol Novolac Epoxy Resin, CNER) (Scheme 1) was chosen for the covalent LbL-assembly at room temperature. Note that during LbL-deposition it is by no means trivial to prevent oligofunctional components from reacting with all of their functional groups

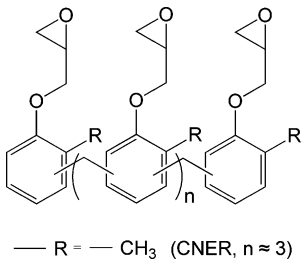

Scheme 1. Chemical structure of the CNER epoxy resin.

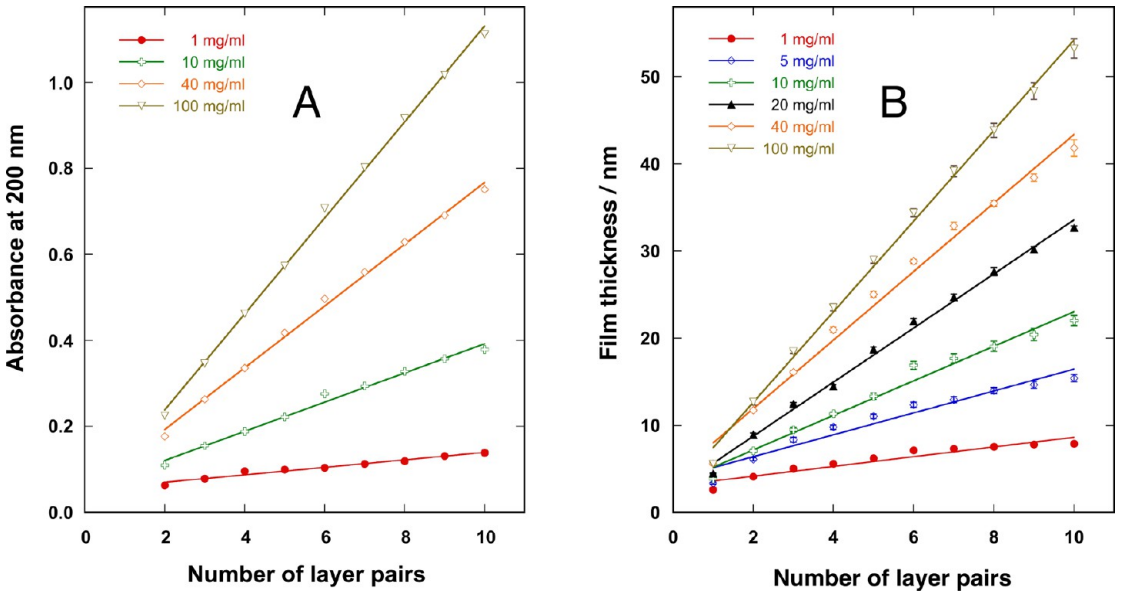

Figure 1. Build-up of LbL-assembled films containing the epoxy resin CNER as a function of the number of layer pairs and of the polymer concentration. The optical absorbance at 220 nm arising from the cresol chromophores of CNER was determined on quartz plates (A) and the corresponding film thickness was determined ellipsometrically on silicon wafers (B). The film architecture is denoted as $(PEI/CNER)_n$ where *n* is the number of layer pairs.

when arriving at the surface, thus rendering the surface nonfunctional and preventing further layer growth. Therefore, it is a key prerequisite to control the chemisorption of each individual layer in a way that the newly arriving moieties in each layer do not adsorb with all their functional groups binding to the surface below. As for noncovalent case of LbL-assembly, conditions must be found (chemical composition, degree of polymerization, concentrations, adsorption times, *etc.*) at which covalently assembled components chemisorb onto the surface with only some of their functional groups bound to the surface while exposing the remaining functional groups to the solution interface.

Construction and Optimization of Epoxy-Based LbL-Films. Various concentrations of PEI and CNER were employed during the optimization stage. The optical absorbance at 220 nm of $(PEI/CNER)_n$ films increases linearly as a function of number of layer pairs deposited on a quartz slide (Figure 1A). The band at 220 nm corresponds to the cresol group of CNER, and a set of the original UV-spectra is shown in the Supporting Information. When such films are deposited on silicon wafers, a linear increase of the film thickness is observed by ellipsometry (Figure 1B). The growth increment for a single layer pair increases with increasing polymer concentration from 0.45 nm for 1 mg/mL to 6.22 nm for 100 mg/mL.

In addition to the effect of polymer concentrations on the growth behavior, effect of adsorption time was also studied (Figure 2). As expected, the film thickness increases both with increasing polymer concentration and with increasing adsorption times. However, at high concentrations and at high adsorption times, films tend to become less homogeneous and require more

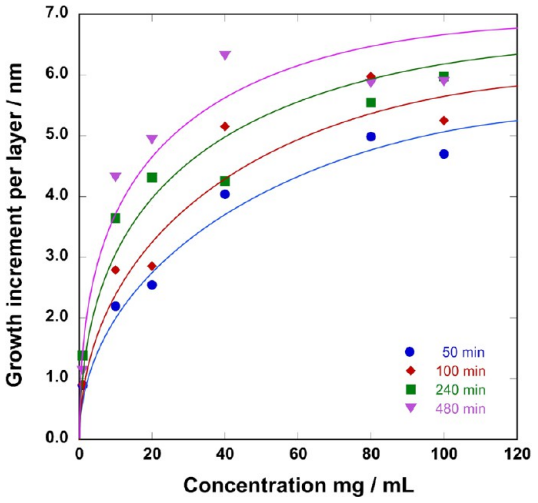

Figure 2. Growth increment per layer of $(PEI/CNER)_n$ films as a function of polymer concentration and time of adsorption. The adsorption times per layer are 50, 100, 240, and 480 min; the solid lines have no physical meaning and are a guide to the eye only.

rinsing. We attribute this behavior to the increasing viscosity of the solutions and to increasing side reactions at long adsorption times as the film deposition was carried out without inert gas. On the basis of these observations, a polymer concentration of 40 mg/mL and an immersion time of 100 min per layer pair (*i.e.*, 50 min per layer) were identified as best conditions for the construction $(PEI/CNER)_n$ multilayer films. These conditions were used for all further experiments.

We have chosen a mechanical rubbing test in which a felt-covered rotating cylinder is pressed against the coated surface (Si-wafer), which is moved at fixed speed in the opposite direction with respect to the

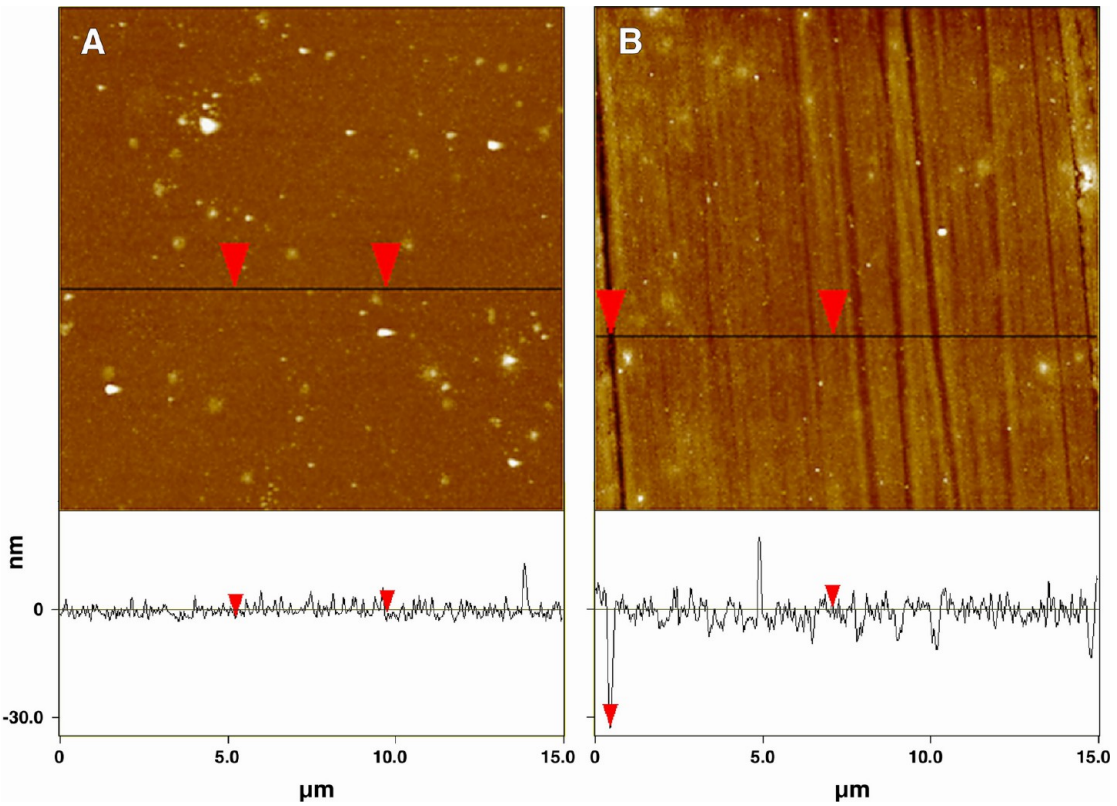

Figure 3. Surface morphology images of $(PEI/CNER)_{10}$ film before rubbing tests (A) and after 60 rubbing cycles (B) obtained by tapping mode AFM. Both images are height images. The traces below correspond to the height profiles taken at the black lines that are shown in the images.

sense of rotation of the cylinder. The device is similar to machines that are used for preparing so-called alignment layers for liquid crystals. Epoxy-based LbL-films demonstrate excellent mechanical resistance against abrasion by such a rubbing machine. Figure 3 shows the atomic force microscopy (AFM) morphology analysis of a $(PEI/CNER)_{10}$ film before and after rubbing test.

Virgin $(PEI/CNER)_{10}$ films have a quite homogeneous surface morphology with a small surface roughness (Figure 3A). After 60 consecutive rubbing cycles, only some trenches appeared on the film surface (Figure 3B), indicating that the changes in surface morphology before and after the rubbing test are small. Comparison of the ellipsometrically determined film thicknesses before and after 60 consecutive rubbing cycles showed an abrasion of the film of about 25−30%, revealing a surprising stability even of very thin epoxy-based LbL-films.

Preparation of Mechanically Weak Functional LbL-Films. An obvious application of covalently assembled LbL-films of epoxy components arises, therefore, from the mechanical robustness of such materials. It is therefore interesting to use such epoxy layers for the mechanical protection of weaker LbL-layers assembled below. In the field of functional LbL-films, particularly soft multilayers are obtained from gold nanoparticles and poly(allylamine hydrochloride).[4,31] Not only are such films mechanically feeble, but they are also of particular interest for preparing nanoplasmonic devices, which need to be robust enough for any application. Freshly prepared films of these components can be effortlessly wiped off a surface with a few rubs.

During the assembly of LbL-films containing the gold nanoparticles, film architectures of the type Si/PEI/PSS/$(PAH/AuNP)_n$/(PAH/PSS) (PSS, poly(sodium 4-styrenesulfonate)) were prepared. The film growth was monitored by UV−vis spectroscopy and ellipsometry (Figure 4A). The ellipsometric data for the $(PAH/AuNP)_5$ film indicated a linear growth as a function of number of layer pairs despite a considerable absorbance of the film at the wavelength of the HeNe laser of the ellipsometer. Since the optical absorbance at the maximum intensity of the AuNP plasmon band of the AuNP films also demonstrated very clearly a linear film growth as a function of the number of deposition cycles, we refrained from using spectroscopic ellipsometry and correcting for the optical absorbance of AuNP films with a dedicated model. Also, for the purpose of this article, it is not required to compare absolute thickness values, and a comparison of relative thickness values is entirely sufficient. The bathochromic shift observed with $(PAH/AuNP)_5$ films with respect to the absorbance of gold nanoparticles in suspension is related to the strong plasmonic coupling between adjacent AuNP layers since they are only separated by a single layer of PAH.

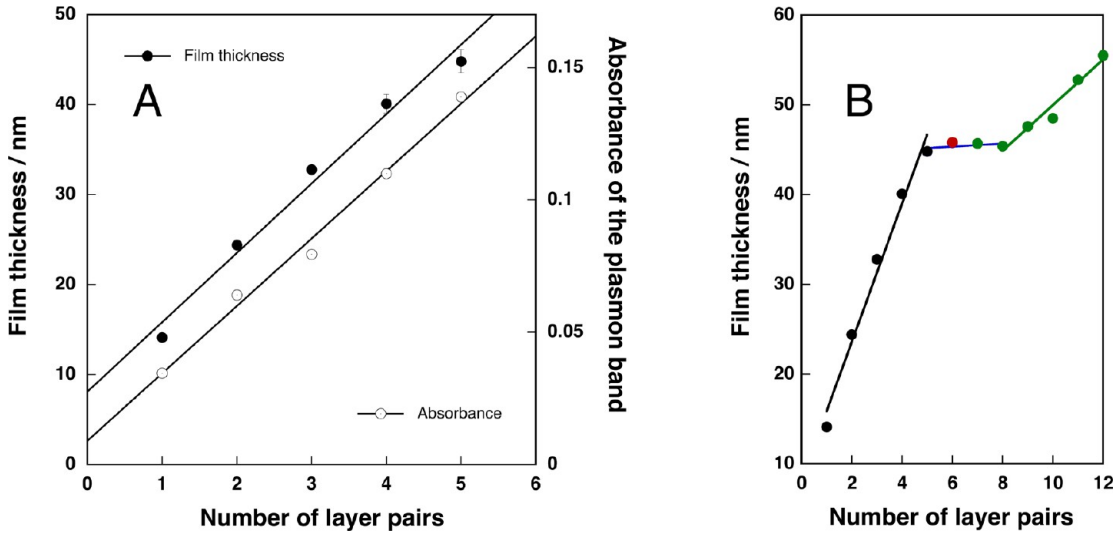

Figure 4. Construction of $(PAH/AuNP)_5$ films on Si wafers and on quartz slides. (A) Ellipsometric film thickness (on Si wafers) and optical absorbance at the position of maximum intensity of the AuNP plasmon band (on quartz slides) and (B) film thickness development for the whole film build-up (weak functional layer (black), intermediate (PSS/PAH) layer pair (red) and protective layer (green) on Si wafers. The lines are linear numerical fits to the corresponding parts of the respective growth regimes. Note that there is no apparent increase of the ellipsometric film thickness (within the experimental error, blue line connecting layer pairs 5 to 8) from the deposition of the last colloidal layer (layer pair 5) until the deposition of the second protective layer pair (layer pair 8).

Protection of Mechanically Weak LbL-Films with a Robust Nanoscale LbL-Coating. Finally, the functional multilayers containing AuNPs were protected with a nanoscale coating of the epoxy-based LbL-films described above. Here it is particularly interesting to determine the smallest number of protective LbL-layers that must be assembled on top of the mechanically weak functional film below in order to provide a desirable mechanical protection.

Judging from the performance of simple $(PEI/CNER)_{10}$ films, two different epoxy-based film architectures were selected as protective coatings, $(PEI/CNER)_3$ and $(PEI/CNER)_6$. The growth of $(PEI/CNER)_n$ layers on top of $Si/PEI/PSS/(PAH/AuNP)_5(PAH/PSS)$ films was also monitored by ellipsometry (Figure 4B). The concentrations of both the polymer solutions were 40 mg/mL with 50 min dipping time in each polymer solution. The film thickness of $(PEI/CNER)_n$ layers on top of $Si/PEI/PSS/(PAH/AuNP)_5(PAH/PSS)$ films increases slowly in the beginning followed by a more pronounced increase at higher layer numbers as shown in Figure 4B. The growth increment of $(PEI/CNER)_n$ layers on top of $Si/PEI/PSS/(PAH/AuNP)_5(PAH/PSS)$ films is 2.1 nm per layer pair and thus somewhat smaller than that for $(PEI/CNER)_n$ films (about 3.6 nm per layer pair) grown on silicon wafers at the same conditions. Such phenomena are not unusual and have been observed before when depositing a certain architecture of a LbL-film on top of a different one.

Analysis of Surface Morphology after Rubbing. The mechanical robustness of all thin films was tested with a rubbing machine already briefly described above. As before, after each rubbing experiment (consisting of up to 60 rubbing cycles), the silicon wafer with the respective LbL-architecture was washed with acetone to remove any loose material and dried. The film thickness before and after the rubbing tests was measured by ellipsometry. Simple $Si/PEI/PSS/(PAH/AuNP)_5/PAH$ films prepared by spray-assisted assembly were tested first and characterized by ellipsometry and AFM before and after mechanical rubbing.

Already after one rubbing cycle, the virgin colloid film had lost 10% of its initial film thickness, and after 5 rubbing cycles, over 90% of the film was removed from the substrate, showing the poor mechanical resistance of virgin AuNP films (Figure 5).

The surface morphology of the virgin colloid film was quite homogeneous with a root-mean-square (rms) roughness of 6.7 ± 0.5 nm at a scanning size of 15 μm (Figure 5A). After only one rubbing cycle, some trenches of varying width appeared on the surface (Figure 5B), whereas the surface roughness barely changed. The slight decrease of the surface roughness of the rubbed film can likely be explained by a palette-knife effect, which could make a film smoother during rubbing. Upon continued rubbing, the surface of the colloid film was progressively eroded by more and more trenches that appeared until the entire film was removed.

For the mechanical protection of AuNP films, the following two different architectures were chosen: $[PEI/PSS/(PAH/AuNP)_5/PAH/PSS]/[PEI/CNER]_3$ and $PSS/(PAH/AuNP)_5/PAH/PSS]/[PEI/CNER]_6$.

For both architectures, the thickness of the colloid film was kept constant.

Figure 6 shows the variation of the film thickness of unprotected and epoxy-protected AuNP colloid films

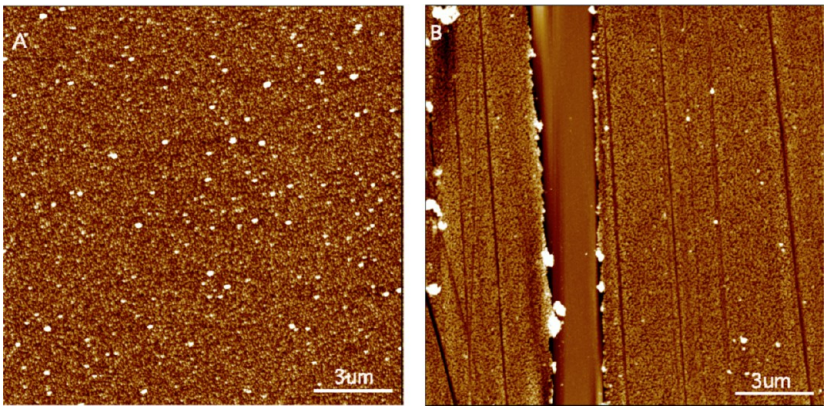

Figure 5. Tapping mode AFM morphologies of Si/PEI/PSS/(PAH/AuNP)$_5$/PAH LbL-films before (A) and after 1 rubbing cycle (B). RMS roughnesses were 6.7 ± 0.5 nm (A) and 5.2 ± 0.3 nm (B); both (A) and (B) are height images.

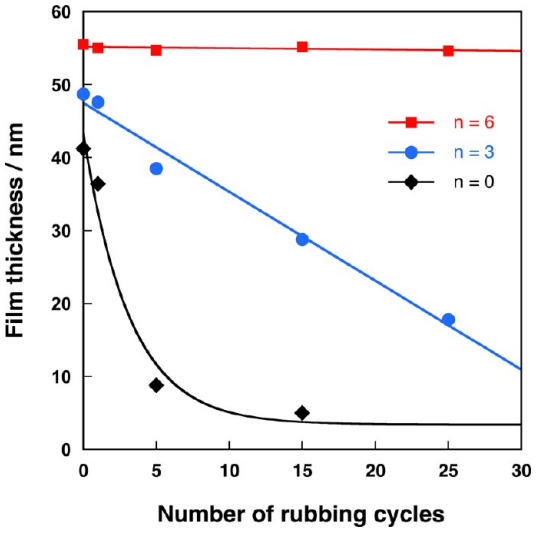

Figure 6. Evolution of the film thicknesses for unprotected (black ◆) and nanoprotected (blue ●, 3 layer pairs; red ■, 6 layer pairs) AuNP-films as a function of different numbers of rubbing cycles. *n* denotes how many layer pairs were used for the protective coating (*n* = 0 no protective coating, the black line corresponds to a numerical fit with a simple exponential decay function; *n* = 3 protective coating with a thickness of about 2 nm, the blue line corresponds to a linear numerical fit; *n* = 6 protective coating with a thickness of about 10 nm, the red line corresponds to a linear numerical fit).

after different numbers of rubbing cycles. As compared to the virgin colloid film, the data clearly show that the presence of an epoxy film improves the mechanical resistance of the colloid film substantially. As expected, the mechanical robustness of the entire sandwich architecture depends on the thickness of the protective epoxy-based film. After 25 rubbing cycles, the thickness of the [PEI/PSS/(PAH/AuNP)$_5$/PAH/PSS]/[PEI/CNER]$_6$ film remains essentially unchanged, whereas the thickness of the [PEI/PSS/(PAH/AuNP)$_5$/PAH/PSS]/[PEI/CNER]$_3$ film decreased considerably. The precise percentages for the remaining thicknesses of the films after 25 rubbing cycles were 98% for the thicker protective coating and 36% for the thinner protective coating (100% refers to the film thickness before rubbing). In addition, films were investigated by AFM (Figure 7) in order to obtain morphological data.

Figure 7 shows representative 20 μm × 20 μm scans of the surface of sandwich films. Note that the film on the left was rubbed only 5 times whereas the film on the right was rubbed 25 times. While both films show that abrasion occurs by forming trenches, there are big differences between the surface morphologies of sandwich films with a different thickness of the protective layer. The [PEI/PSS/(PAH/AuNP)$_5$/PAH/PSS]/[PEI/CNER]$_3$ film was completely torn up after 5 rubbing cycles, so further rubbing was stopped for this particular sample. The dark trench in Figure 7A likely corresponds to the PEI layer or the silicon substrate as judging from the thickness of the original film in comparison with the depth of the trench. The AFM-based surface roughness indicates a RMS value of 3.4 ± 0.6 nm for the (PEI/PSS/(PAH/Au)$_5$/PAH/PSS]/[PEI/CNER]$_3$ film before the rubbing test, which is similar to the value obtained for a simple (PEI/CNER)$_{10}$ film (2.9 nm). After 5 rubbing cycles, the surface roughness increases to 10.7 nm (Figure 7A).

Even after 5 times more rubbing cycles, the [PEI/PSS/(PAH/AuNP)$_5$/PAH/PSS]/[PEI/CNER]$_6$ films show much less damage than sandwich films with the thinner protective coating; their morphology looks very similar to that of simple (PEI/CNER)$_{10}$ films after 60 rubbing cycles (Figure 3B). The trench with red markers has a vertical distance of 55.5 nm (Figure 7B), which corresponds well to the thickness of the [PEI/PSS/(PAH/AuNP)$_5$/PAH/PSS]/[PEI/CNER]$_6$ film.

SUMMARY AND CONCLUSIONS

One of the most important benefits of layer-by-layer assembly arises from the ease by which different materials can be combined in a single device ("multimaterial assembly"). Here it has been demonstrated that the abrasion resistance of functional but mechanically weak films can substantially be increased by very thin coatings composed of components with established mechanical toughness. A LbL-film with a thickness of about 45 nm composed of gold

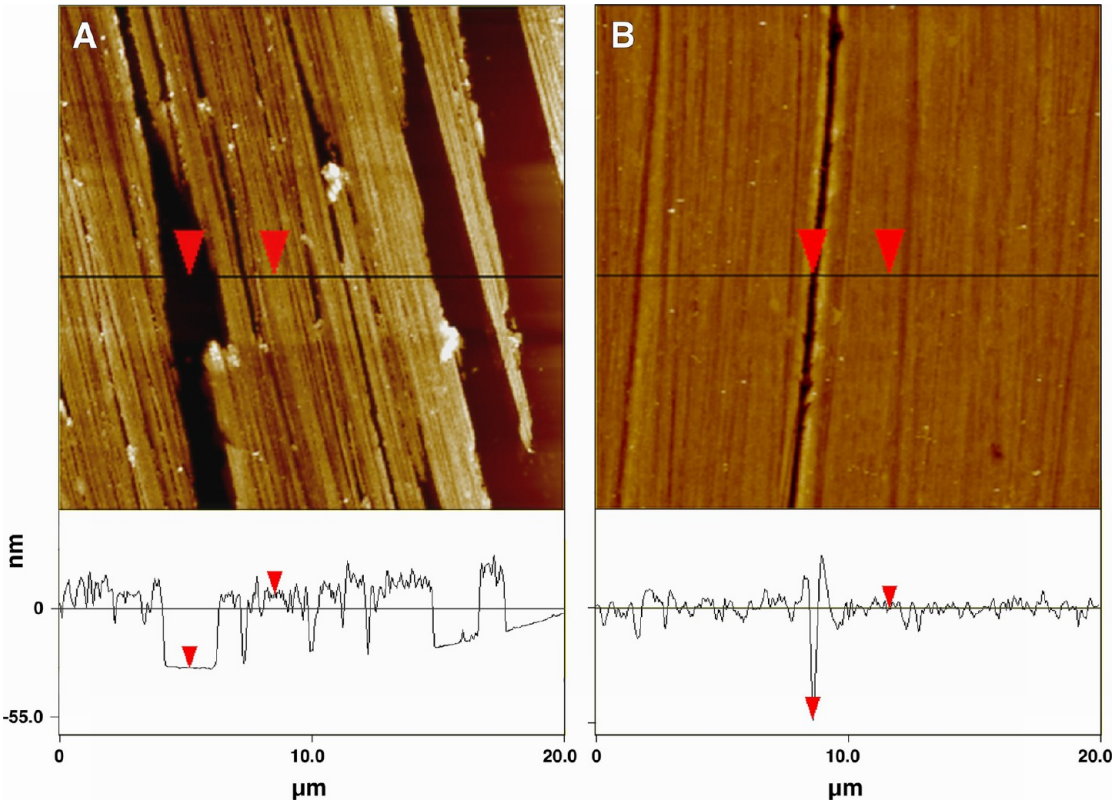

Figure 7. Surface morphology images of epoxy protected AuNP films (A) [PEI/PSS/(PAH/AuNP)$_5$/PAH/PSS]/[PEI/CNER]$_3$ film, after 5 rubbing cycles and (B) [PEI/PSS/(PAH/AuNP)$_5$/PAH/PSS]/[PEI/CNER]$_6$ film, after 25 rubbing cycles as observed by tapping mode AFM. All images are height images. The step heights determined by AFM (corresponding to the film thicknesses after rubbing, about 38 nm for (A) and about 55 nm for B) are consistent with the film thicknesses determined by ellipsometry after rubbing (Figure 6).

nanoparticles and poly(allylamine hydrochloride) was chosen as an especially weak example for a functional multilayer system; similar films might be used, for example, in plasmonic devices. In the present work, a classic epoxy binder (CNER) was co-assembled with a water-soluble polyamine (PEI) to form thin protective layers on top of the functional layer. After optimizing the preparation conditions for such films, the thickness of the protective coating was controlled by building-up either 3 or 6 layer pairs of (PEI/CNER) through covalent LbL-deposition at ambient temperature. First, the abrasion resistance of simple (PEI/CNER) films was tested using a conventional rubbing machine and found to be greatly enhanced in comparison to that of many LbL-films that were prepared through electrostatic interactions. Then, the ability of such films to act as protective coating for mechanically weak layers below was qualitatively evaluated. For the abrasion test used here, the critical thickness for a protective LbL-coating on top of the weak multilayer is about 6 layer pairs corresponding to only about 10 nm. At this thickness, the entire film withstands at least 25 rubbing cycles with a reduction of the total thickness of about 2% or less. Note that it is by no means trivial to prepare homogeneous ultrathin epoxy films as epoxy components frequently show surface induced phase separation due to wetting phenomena. This present work also opens up opportunities to extend the preparation of nanoprotective LbL-coatings to water-soluble epoxides or other types of chemically cross-linked materials.

METHODS

Polymers and Solutions. Poly[(*o*-cresyl glycidyl ether)-*co*-formaldehyde] (trade name Cresol Novolac Epoxy Resin (CNER), $\bar{M}_n \approx 1270$ g/mol, batch 06527MI) was purchased from Sigma Aldrich (Lyon, France) and used without further purification.

Poly(sodium 4-styrenesulfonate) (PSS, $\bar{M}_w \approx 70\,000$ g/mol, batch PI06005MU), poly(allylamine hydrochloride) (PAH, $\bar{M}_w \approx 70\,000$ g/mol, batch 05212MO-083) and branched poly(ethylenimine) (PEI, $\bar{M}_w < 25\,000$ g/mol, batch 09620EA-193) were purchased from Aldrich (Lyon, France) and used without further purification.

Epoxy solutions were prepared in acetone (99.5%, Sigma-Aldrich, Lyon, France) while PSS, PAH, and PEI solutions were prepared using ultrapure water (Milli-Q Gradient system, Millipore, Molsheim, France) with a resistivity of 18.2 MΩ·cm. PEI and CNER solutions were prepared at concentrations of 1, 10, 20, 40, 80, and 100 mg/mL, while PSS and PAH were prepared at concentrations 0.6 and 0.27 mg/mL, respectively. Each polyelectrolyte, except PEI, was dissolved in Milli-Q water containing 0.5 M sodium chloride (NaCl, ≥ 99.5%, batch

096K0076, Sigma, Lyon, France), whereas PEI was dissolved in Milli-Q water.

Synthesis of Gold Nanoparticles (AuNPs). Gold(III) chloride trihydrate (≥49.0% Au basis, batch 066K1440) and sodium citrate dihydrate (≥99%, batch S05962-061) were purchased from Sigma-Aldrich (Lyon, France). AuNPs were synthesized as described previously using the standard reduction of tetrachloroauric(III) acid ($HAuCl_4 \cdot 3H_2O$) with sodium citrate.[32] AuNPs were used within a few days after their synthesis.

Substrate Preparation. Silicon wafers with an orientation (100) were purchased from Wafernet, Inc. (San José, CA). All wafers were cut to a size of about 12 mm × 45 mm for film construction and 25 mm × 75 mm for rubbing tests. Suprasil quartz slides were purchased from Hellma (Paris, France).

Prior to film deposition, all substrates were cleaned in a 1:1 (v/v) mixture of methanol (CH_3OH, 99.9%, batch 0604772 BDH, Prolabo) and hydrochloric acid (HCl 37%, Sigma-Aldrich, Lyon, France) for 30 min and then stored overnight in a concentrated sulfuric acid solution (H_2SO_4, 95−97%, batch 63280, Sigma-Aldrich, Lyon, France). Prior to use, each substrate was extensively rinsed with Milli-Q water and dried under a stream of nitrogen.

All chemical products mentioned above were used without further purification.

Ellipsometry. Measurement of the film thickness was carried out with a PLASMOS SD2100 instrument operating at a single wavelength of 632.8 nm (He/Ne laser) and a constant angle of 70°. The refractive index of all polymer films was assumed to be constant at $n = 1.465$. This procedure leads to slightly incorrect values with respect to the absolute film thickness, but it allows for a quick determination of the relative film thickness. Thickness values obtained with the assumption of a fixed refractive index for all films are of better precision than required for the comparison of film growth data as in this report. For each substrate studied, 10 points were randomly measured to obtain the average value for the film thickness and to determine the film homogeneity.

UV−Visible Spectroscopy. UV−visible spectra of films prepared on quartz slides were recorded on a Varian Cary 500 Scan spectrometer. The changes of the spectral intensities due to light absorption by either aromatic groups of CNER, AuNPs and/or PSS within the films were used to follow the evolution of the film thickness.

Atomic Force Microscopy (AFM). AFM images were obtained in tapping mode with a Multimode Nanoscope IIIA Scanning Probe Microscope from Veeco (Santa Barbara, CA) and noncoated silicon cantilevers (Veeco, model TAP150, $k = 5$ N/m, $f_0 = 68-132$ kHz). Deflection and height mode images were scanned simultaneously at a fixed scan rate with a resolution of 512 × 512 pixels. All scans were repeated several times in order to ensure reproducibility and to rule out surface damage.

Mechanical Abrasion. The mechanical abrasion tests of LbL-films were carried out with a home-build apparatus described elesewhere.[33] In brief, a cylinder (4 cm diameter) covered with a microfiber cloth and rotating at a constant speed was pressed at ambient temperature with a constant pressure of 2 bar against a horizontally mounted LbL-film that was moved by a translation stage at constant speed opposite to the rotation direction of the cylinder. The brushing cycles were automated and electropneumatically controlled. The rubbing operating conditions were identical for all experiments.

Covalent Layer-by-Layer Assembly of Epoxy-Based Films. For film build-up, the thickness of the cleaned silicon wafer was first measured by ellipsometry. This "base"-thickness of the SiO_2 layer was later subtracted from the thickness measurements at various stages of film growth to obtain the thickness of the multilayer films.

The substrate was then dipped in aqueous PEI solution for time $t_1 = 25$, 50, 120, 180, or 240 min, followed by rinsing in pure water (t_2). The rinsing was done by dipping the substrate for 2 min each in three different beakers, each containing 15 mL of Milli-Q water, in order to remove the excess of PEI from the surface. The substrate was subsequently dried in a stream of pure nitrogen gas and dipped in the CNER solution prepared in acetone for time $t_3 = t_1$, followed by rinsing in pure acetone (t_4). Rinsing was carried out by consecutively immersing the substrate for 2 min each in three beakers each containing 15 mL of pure acetone, in order to remove excess CNER from the surface. After the film was dried in a stream of pure nitrogen gas, measurements by ellipsometry were carried out to determine the film thickness of the layer pair. A multilayer film composed of n PEI and CNER layer pairs is denoted as $(PEI/CNER)_n$ where $n = 1-10$ and CNER is always the outermost layer. For a single layer pair, the total deposition time was $t = t_1 + t_2 + t_3 + t_4$.

This procedure was also used to coat cleaned quartz slides for the characterization of $(PEI/CNER)_n$ film growth by UV−vis spectrometry.

Spray-Assisted Deposition of $(PAH/AuNP)_n$ Films. $(PAH/AuNP)_n$ multilayer films were assembled by spraying after the deposition of a PEI precursor layer. The cleaned Si-wafers were dipped into a PEI solution for 5 min, rinsed in Milli-Q water, and dried under a nitrogen flux prior to deposition by spraying.

The spray-deposition was carried out by using manual spray cans (Roth Sochiel Eurl, Lauterbourg, France) as described before.[34] Different spray cans were used for the PSS, PAH, AuNPs, and the rinsing solution (a 0.5 M aqueous solution of NaCl for PSS and PAH and Milli-Q water for AuNPs). The spray conditions for polymer solutions were as follows: spraying time $t'_1 = 5$ s, contact time $t'_2 = 15$ s, rinsing time $t'_3 = 5$ s, waiting time $t'_4 = 15$ s. To ensure a full surface coverage by AuNPs, the spray conditions used for polymer solution were repeated 5 times for AuNP solution. Thus, the deposition time of a PAH layer was 40 s, while the deposition time of an AuNP layer was 200 s. The total deposition time (t') for a single layer pair deposited by spraying corresponds accordingly to $(6t'_1 + 6t'_2 + 6t'_3 + 6t'_4) = 240$ s. The film growth was monitored by ellipsometry (Si-wafer) and by UV−vis spectroscopy (quartz slide).

Covalent LbL-Assembly of a Protective Epoxy Film on Top of a Mechanically Weak LbL-Film. After the deposition of a Si/PEI/PSS/$(PAH/AuNP)_n$/PAH film on the substrate, a (PSS) layer was deposited by spraying on top of the last PAH layer before the deposition of a $(PEI/CNER)_n$ multilayer by dipping using the procedure described above for the preparation of epoxy-based coatings. The concentration of PEI and CNER solutions was 40 mg/mL.

Conflict of Interest: The authors declare no competing financial interest.

Acknowledgment. We gratefully acknowledge support from the Higher Education Commission (HEC, International Research Support Initiative Program (IRSIP), project number 1-8/HEC/HRD/2006/247 and followup projects), Pakistan, the Ministère de l'Enseignement Supérieur et de la Recherche, France, the Centre National de la Recherche Scientifique (CNRS), France and the Institut Universitaire de France. All authors are indebted to Dr. Martin Brinkmann for providing access to his rubbing machine and for supporting our experiments. The authors acknowledge the help of Christophe Contal with the AFM training and imaging.

Supporting Information Available: UV−visible spectra for $(PEI/CNER)_n$ film build-up as a function of polymer concentration. This material is available free of charge *via* the Internet at http://pubs.acs.org.

REFERENCES AND NOTES

1. Decher, G. Fuzzy Nanoassemblies: Toward Layered Polymeric Multicomposites. *Science* **1997**, *277*, 1232–1237.
2. Decher, G.; Hong, J. D.; Schmitt, J. Buildup of Ultrathin Multilayer Films by a Self-Assembly Process. 3. Consecutively Alternating Adsorption of Anionic and Cationic Polyelectrolytes on Charged Surfaces. *Thin Solid Films* **1992**, *210*, 831–835.
3. Lvov, Y.; Haas, H.; Decher, G.; Möhwald, H.; Mikhailov, A.; Mtchedlishvily, B.; Morgunova, E.; Vainshtein, B. Successive Deposition of Alternate Layers of Polyelectrolytes and a Charged Virus. *Langmuir* **1994**, *10*, 4232–4236.
4. Schmitt, J.; Decher, G.; Dressick, W. J.; Brandow, S. L.; Geer, R. E.; Shashidhar, R.; Calvert, J. M. Metal Nanoparticle/

Polymer Superlattice Films: Fabrication and Control of Layer Structure. *Adv. Mater.* **1997**, *9*, 61–65.
5. Kotov, N. A.; Dekany, I.; Fendler, J. H. Layer-by-Layer Self-Assembly of Polyelectrolyte-Semiconductor Nanoparticle Composite Films. *J. Phys. Chem.* **1995**, *99*, 13065–13069.
6. Kleinfeld, E. R.; Ferguson, G. S. Stepwise Formation of Multilayered Nanostructural Films from Macromolecular Precursors. *Science* **1994**, *265*, 370–373.
7. Kaschak, D. M.; Mallouk, T. E. Inter- and Intralayer Energy Transfer in Zirconium Phosphate Poly(allylamine hydrochloride) Multilayers: An Efficient Photon Antenna and a Spectroscopic Ruler for Self-Assembled Thin Films. *J. Am. Chem. Soc.* **1996**, *118*, 4222–4223.
8. Jessel, N.; Oulad-Abdeighani, M.; Meyer, F.; Lavalle, P.; Haikel, Y.; Schaaf, P.; Voegel, J. C. Multiple and Time-Scheduled *in Situ* DNA Delivery Mediated by Beta-Cyclodextrin Embedded in a Polyelectrolyte Multilayer. *Proc. Natl. Acad. Sci. U.S.A.* **2006**, *103*, 8618–8621.
9. Jayant, R. D.; McShane, M. J.; Srivastava, R. *In Vitro* and *in Vivo* Evaluation of Anti-Inflammatory Agents Using Nanoengineered Alginate Carriers: Towards Localized Implant Inflammation Suppression. *Int. J. Pharm.* **2011**, *403*, 268–275.
10. Kim, B. S.; Smith, R. C.; Poon, Z.; Hammond, P. T. MAD (Multiagent Delivery) Nanolayer: Delivering Multiple Therapeutics from Hierarchically Assembled Surface Coatings. *Langmuir* **2009**, *25*, 14086–14092.
11. Schneider, G. F.; Subr, V.; Ulbrich, K.; Decher, G. Multifunctional Cytotoxic Stealth Nanoparticles. A Model Approach with Potential for Cancer Therapy. *Nano Lett.* **2009**, *9*, 636–642.
12. Lee, D.; Cui, T. J. Layer-by-Layer Self-Assembly of Single-Walled Carbon Nanotubes with Amine-Functionalized Weak Polyelectrolytes for Electrochemically Tunable pH Sensitivity. *Langmuir* **2011**, *27*, 3348–3354.
13. Bergbreiter, D. E.; Liao, K. S. Covalent Layer-by-Layer Assembly-An Effective, Forgiving Way to Construct Functional Robust Ultrathin Films and Nanocomposites. *Soft Matter* **2009**, *5*, 23–28.
14. Buck, M. E.; Zhang, J.; Lynn, D. M. Layer-by-Layer Assembly of Reactive Ultrathin Films Mediated by Click-Type Reactions of Poly(2-alkenyl azlactone)s. *Adv. Mater.* **2007**, *19*, 3951–3955.
15. Chen, J. Y.; Luo, G. B.; Cao, W. X. Fabrication of a Covalently Attached Multilayer Film *via in-Situ* Reaction. *Macromol. Rapid Commun.* **2001**, *22*, 311–314.
16. Fang, M. M.; Kaschak, D. M.; Sutorik, A. C.; Mallouk, T. E. A "Mix and Match" Ionic−Covalent Strategy for Self-Assembly of Inorganic Multilayer Films. *J. Am. Chem. Soc.* **1997**, *119*, 12184–12191.
17. Fu, Y.; Xu, H.; Bai, S. L.; Qiu, D. L.; Sun, J. Q.; Wang, Z. Q.; Zhang, X. Fabrication of a Stable Polyelectrolyte/Au Nanoparticles Multilayer Film. *Macromol. Rapid Commun.* **2002**, *23*, 256–259.
18. Gill, R.; Mazhar, M.; Felix, O.; Decher, G. Covalent Layer-by-Layer Assembly and Solvent Memory of Multilayer Films from Homobifunctional Poly(dimethylsiloxane). *Angew. Chem., Int. Ed.* **2010**, *49*, 6116–6119.
19. Liang, Z. Q.; Dzienis, K. L.; Xu, J.; Wang, Q. Covalent Layer-by-Layer Assembly of Conjugated Polymers and CdSe Nanoparticles: Multilayer Structure and Photovoltaic Properties. *Adv. Funct. Mater.* **2006**, *16*, 542–548.
20. Pastoriza-Santos, I.; Scholer, B.; Caruso, F. Core-Shell Colloids and Hollow Polyelectrolyte Capsules Based on Diazoresins. *Adv. Funct. Mater.* **2001**, *11*, 122–128.
21. Such, G. K.; Tjipto, E.; Postma, A.; Johnston, A. P. R.; Caruso, F. Ultrathin, Responsive Polymer Click Capsules. *Nano Lett.* **2007**, *7*, 1706–1710.
22. Sun, J. Q.; Wu, T.; Sun, Y. P.; Wang, Z. Q.; Zhang, X.; Shen, J. C.; Cao, W. X. Fabrication of a Covalently Attached Multilayer *via* Photolysis of Layer-by-Layer Self-Assembled Films Containing Diazo-Resins. *Chem. Commun.* **1998**, 1853–1854.
23. Zhang, F.; Jia, Z.; Srinivasan, M. P. Application of Direct Covalent Molecular Assembly in the Fabrication of Polyimide Ultrathin Films. *Langmuir* **2005**, *21*, 3389–3395.
24. Zhang, S. X.; Yang, W. W.; Niu, Y. M.; Sun, C. Q. Multilayered Construction of Glucose Oxidase on Gold Electrodes Based on Layer-by-Layer Covalent Attachment. *Anal. Chim. Acta* **2004**, *523*, 209–217.
25. Gemici, Z.; Shimomura, H.; Cohen, R. E.; Rubner, M. F. Hydrothermal Treatment of Nanoparticle Thin Films for Enhanced Mechanical Durability. *Langmuir* **2008**, *24*, 2168–2177.
26. Nuraje, N.; Asmatulu, R.; Cohen, R. E.; Rubner, M. F. Durable Antifog Films from Layer-by-Layer Molecularly Blended Hydrophilic Polysaccharides. *Langmuir* **2011**, *27*, 782–791.
27. Mohan, P. A Critical Review: The Modification, Properties, and Applications of Epoxy Resins. *Polym.-Plast. Technol. Eng.* **2013**, *52*, 107–125.
28. Mateo, C.; Torres, R.; Fernandez-Lorente, G.; Ortiz, C.; Fuentes, M.; Hidalgo, A.; Lopez-Gallego, F.; Abian, O.; Palomo, J. M.; Betancor, L.; Pessela, B. C. C.; Guisan, J. M.; Fernandez-Lafuente, R. Epoxy-Amino Groups: A New Tool for Improved Immobilization of Proteins by the Epoxy Method. *Biomacromolecules* **2003**, *4*, 772–777.
29. Liu, Y. L.; Liu, C. S.; Chen, W. H.; Chen, S. Y.; Wang, K. S.; Hwu, M. J. Ultra-Low-k Thin Films of Polyhedral Oligomeric Silsesquioxane/Epoxy Nanocomposites *via* Covalent Layer-by-Layer Assembly. *J. Nanosci. Nanotechnol.* **2009**, *9*, 1839–1843.
30. Luzinov, I.; Julthongpiput, D.; Liebmann-Vinson, A.; Cregger, T.; Foster, M. D.; Tsukruk, V. V. Epoxy-Terminated Self-Assembled Monolayers: Molecular Glues for Polymer Layers. *Langmuir* **2000**, *16*, 504–516.
31. Lu, C. H.; Donch, I.; Nolte, M.; Fery, A. Au Nanoparticle-Based Multilayer Ultrathin Films with Covalently Linked Nanostructures: Spraying Layer-by-Layer Assembly and Mechanical Property Characterization. *Chem. Mater.* **2006**, *18*, 6204–6210.
32. Schneider, G.; Decher, G. From Functional Core/Shell Nanoparticles Prepared *via* Layer-by-Layer Deposition to Empty Nanospheres. *Nano Lett.* **2004**, *4*, 1833–1839.
33. Brinkmann, M.; Pratontep, S.; Chaurnont, C.; Wittmann, J. C. Oriented and Nanostructured Polycarbonate Substrates for the Orientation of Conjugated Molecular Materials and Gold Nanoparticles. *Macromolecules* **2007**, *40*, 9420–9426.
34. Izquierdo, A.; Ono, S. S.; Voegel, J. C.; Schaaf, P.; Decher, G. Dipping *versus* Spraying: Exploring the Deposition Conditions for Speeding up Layer-by-Layer Assembly. *Langmuir* **2005**, *21*, 7558–7567.